

Supporting Information

Pump-Probe X-ray Solution Scattering Reveals Accelerated Folding of Cytochrome *c* Upon Suppression of Misligation[†]Tae Wu Kim,^{‡,§} Jong Goo Kim,^{‡,§} Cheolhee Yang,^{‡,§} Hosung Ki,^{‡,§} Junbeom Jo,^{‡,§} and Hyotcherl Ihee^{‡,§,*}[‡]Department of Chemistry, Korea Advanced Institute of Science and Technology (KAIST), Daejeon 305-701, Korea[§]Center for Nanomaterials and Chemical Reactions, Institute for Basic Science (IBS), Daejeon 305-701, Korea

*E-mail: hyotcherl.ihee@kaist.ac.kr

Received August 3, 2013, Accepted August 24, 2013

Experimental Details

Horse heart cytochrome *c* (Cyt *c*) purchased from Sigma-Aldrich was dissolved in 100 mM of Na-phosphate and 4 M of guanidine hydrochloride at pH 7. A centrifuge with the cellulose acetate membrane filter was used to remove the aggregated particles. After adding sodium dithionite to the aggregation-free Cyt *c* solution, it was bubbled using CO gas for 30 minutes. The protein concentration determined using the absorption spectrum was 4.4 mM. For the sample with imidazole, the buffer contained 200 mM of imidazole; otherwise, the procedure for the sample preparation was identical regardless of the presence of imidazole. The pump-probe (time-resolved) X-ray solution scattering data were measured with 1.5 μ s time resolution using X-ray pulses produced from the 324-bunch mode operation in the BioCARS 14-ID-B beamline at the Advanced Photon Source.¹ The previously established experimental protocol was followed.²⁻⁵ The solution of Cyt *c* bound with CO in a quartz capillary was excited using a \sim 10 ns laser pulse at 532 nm generated from the OPO setup and 1 mJ/mm² of fluence in order to dissociate CO from Cyt *c* bound with CO. Subsequently, a \sim 1.5 μ s X-ray pulse probed the sample at well-defined time delays with respect to the arrival of the laser pulse. The scattered X-rays were recorded in a Mar165 CCD detector (Rayonix, USA) as a function of the time delay between the laser and X-ray pulses. During the measurement, the spatial overlap between the laser and X-ray, and the energy density of the laser were periodically checked in order to guarantee the maximum quantum yield for the CO photodissociation.

Singular Value Decomposition (SVD) Analysis

From the experimental scattering curves measured at various time delays, an $n_q \times n_t$ data matrix can be built where n_q is the number of q points in the difference scattering curve at a given time delay point and n_t is the number of time delay

points. In this work, n_q and n_t are 266 and 9, respectively. This matrix (A) can be decomposed while satisfying the relationship of $A=USV^T$, where U is an $n_q \times n_t$ matrix whose columns are left singular vectors (LSVs; corresponding to the time-independent q spectra) of A , V is an $n_t \times n_t$ matrix whose columns are right singular vectors (rSVs; corresponding to the amplitude change of U as time progresses) of A , and S is a diagonal $n_t \times n_t$ matrix whose diagonal elements are singular values of A . The matrices U and V have the properties of $U^T U = I_{n_t}$ and $V^T V = I_{n_t}$, respectively, where I_{n_t} is the identity matrix. Since the diagonal elements (*i.e.* singular values) of S , which represents the weight of the left singular vectors in U , are ordered so that $s_1 \geq s_2 \geq \dots \geq s_n \geq 0$, both the left and right singular vectors on more left are supposed to have larger contributions to the constructed experimental data. In this manner, the time-independent scattering intensity components can be extracted from the left singular vectors and the time evolution of their amplitudes from the right singular vectors⁶⁻⁸ (Figure S1a and Figure 1(c)). When combined, the former can provide information on the scattering curves of distinct transient species (intermediates), while the latter contains information on the population dynamics of the transient species.

In order to determine the significant components of the LSVs and rSVs, the singular values of A and the autocorrelation values of rSVs are considered. In general, the meaningful tendency of the amplitude change in the rSVs demonstrates an autocorrelation value close to unity. Based on both the singular values and the autocorrelation values, a significant contribution is clear for the first two singular vectors and the third singular vector also may contain meaningful information for both samples with and without imidazole (Figures S1a and S1b). The first two rSVs were used to determine the apparent rate constants.

The apparent rate constants are extracted through fitting the right singular vectors to the sum of exponentials. Three exponentials ($\tau = 40 (\pm 4) \mu$ s, $2.3 (\pm 0.2)$ ms, and $37 (\pm 9)$ ms) were used to simultaneously fit the right singular vectors for the sample without imidazole (see Figure 1(c)). However, in the presence of imidazole, the two exponentials ($367 (\pm 230) \mu$ s, and $56 (\pm 41)$ ms) were sufficient to describe the

[†]This paper is to commemorate Professor Myung Soo Kim's honourable retirement.

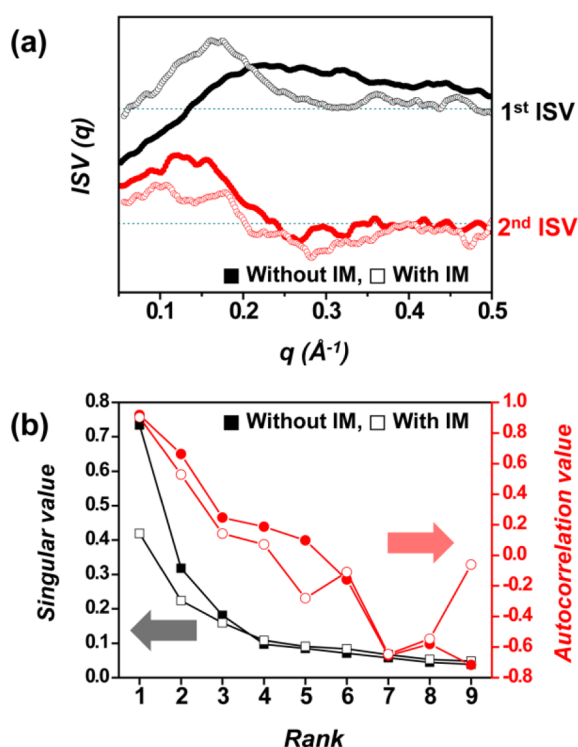


Figure S1. (a) The first (black) and second (red) left singular vectors (ISVs) extracted from the SVD analysis. The filled and empty symbols indicate the absence and presence of imidazole (IM), respectively. (b) Singular values (black) and autocorrelation values (red).

amplitude changes of the right singular vectors (see Figure 1(c)). Based on the fit of the significant right singular vectors for each data, the effect of imidazole on suppressing the misligation between the His26/33 and iron on the heme is clearly observed in view of the kinetic components.

References

1. Graber, T.; Anderson, S.; Brewer, H.; Chen, Y. S.; Cho, H. S.; Dashdorj, N.; Henning, R. W.; Kosheleva, I.; Macha, G.; Meron, M.; Pahl, R.; Ren, Z.; Ruan, S.; Schotte, F.; Rajer, V. S.; Viccaro, P. J.; Westferro, F.; Anfinrud, P.; Moffat, K. *J. Synchrotron Radiat.* **2011**, *18*, 658.
2. Kim, T. W.; Lee, J. H.; Choi, J.; Kim, K. H.; van Wilderen, L. J.; Guerin, L.; Kim, Y.; Jung, Y. O.; Yang, C.; Kim, J.; Wulff, M.; van Thor, J. J.; Ihee, H. *J. Am. Chem. Soc.* **2012**, *134*, 3145.
3. Kim, K. H.; Muniyappan, S.; Oang, K. Y.; Kim, J. G.; Nozawa, S.; Sato, T.; Koshihara, S. Y.; Henning, R.; Kosheleva, I.; Ki, H.; Kim, Y.; Kim, T. W.; Kim, J.; Adachi, S.; Ihee, H. *J. Am. Chem. Soc.* **2012**, *134*, 7001.
4. Kim, J.; Kim, K. H.; Kim, J. G.; Kim, T. W.; Kim, Y.; Ihee, H. *J. Phys. Chem. Lett.* **2011**, *2*, 350.
5. Cammarata, M.; Levantino, M.; Schotte, F.; Anfinrud, P. A.; Ewald, F.; Choi, J.; Cupane, A.; Wulff, M.; Ihee, H. *Nat. Methods* **2008**, *5*, 881.
6. Schmidt, M.; Pahl, R.; Srajer, V.; Anderson, S.; Ren, Z.; Ihee, H.; Rajagopal, S.; Moffat, K. *Proc. Natl. Acad. Sci. USA* **2004**, *101*, 4799.
7. Ihee, H.; Rajagopal, S.; Srajer, V.; Pahl, R.; Anderson, S.; Schmidt, M.; Schotte, F.; Anfinrud, P. A.; Wulff, M.; Moffat, K. *Proc. Natl. Acad. Sci. USA* **2005**, *102*, 7145.
8. Henry, E. R.; Hofrichter, J. *Method Enzymol.* **1992**, *210*, 129.